

SIMULATION OF AIR FLOW AND DEHYDRATION PROCESS IN TRAY DRYING SYSTEMS

Adrian-Gabriel GHIAUS¹, Robert GAVRILIUC²

Uscătoarele, ca mari consumatoare de energie, necesită o optimizare reală bazată pe modele matematice dinamice, analize și simulări numerice. Comportarea sistemului este direct influențată de viteza aerului deasupra produsului (care se modifică datorită contracției produsului), de proprietățile termo-fizice ale produsului variabile în timp cu temperatura și umiditatea, ca și de coeficienții de transfer și de proprietățile aerului de uscare. Curgerea aerului în interiorul camerei de uscare este investigată cu ajutorul unui cod C.F.D. Simularea curgerii pentru diferite configurații geometrice, prezintând diagrame cu linii de curent, vectori de viteză și distribuția presiunii, impune utilizarea aranjamentului corect.

Drying systems, as great energy consumers, need an actual optimization based on dynamic mathematical models, analysis and numerical simulations. The system behaviour is direct influenced by the air velocity above the product bed (which change due to the product shrinkage), by the thermo-physical properties of the product depending on temperature and moisture content - variable in time, as well as by the transfer coefficients and drying air properties. The air flow inside the drying room is investigated by means of well established C.F.D. code. Flow simulation for different geometrical configurations, showing stream lines, velocity vectors and pressure distribution diagrams, dictate the right arrangement to be used.

Keywords: Batch drying units; drying process; tray dryer; numerical simulation

1. Introduction

Phase separation processes are often associated with industrial units having complex geometry configuration. Whenever a fluid is involved in a separation process, the main factor that affects the overall system efficiency is the flow behaviour. In the case of fluid passages having complicated geometry aspect, the use of Computational Fluid Dynamics (CFD) codes is a convenient way to evaluate the gas flow parameters. However, to obtain trustful results from numerical simulations, the codes have to be validated by means of experimental measurements.

¹ Reader, Department of Thermal Engineering, Technical University of Civil Engineering, Bucharest, ROMANIA

² Prof., Department of Thermal Engineering, Technical University of Civil Engineering, Bucharest, ROMANIA

Experimental fluid dynamics has played an important role in validating and delineating the limits of the various approximations to the governing equations. For example, wind tunnels provide an effective means of reproducing actual flows at laboratory scale. Traditionally, this has conferred a cost effective alternative to full-scale measurement. However, in the design of such equipment that critically depends on the flow behaviour (e.g. in phase separation processes), as part of the design process, measurements are economically impractical. On the other hand, the use of Computational Fluid Dynamics codes leads to numerical solutions of the governing equations and to a complete description of the flow field of interest.

One of the biggest requirements in drying processes is the achievement of uniform moisture content of the final product. This becomes more difficult for large batch drying systems used especially for dehydration of agricultural products. Uniformity of the moisture content inside the final product could be obtained through a proper distribution and guidance of the drying air inside the drying space [1]. This implies the insertion of special devices that will complicate even more the geometry of the space where the flow is developed.

For the case presented in this paper, numerical simulation is carried out using the well-known PHOENICS CFD code in order to predict the airflow parameters and to optimise the design of the dryer.

2. Mathematical modelling of the flow

In a general form, the transport equation for momentum, kinetic energy, dissipation rate, etc. can be written as:

$$\frac{\partial}{\partial t}(\rho \Phi) + \operatorname{div}(\rho \vec{w} \Phi) = \operatorname{div}(\Gamma_\Phi \operatorname{grad}(\Phi)) + S_\Phi \quad (1)$$

transient + convection = diffusion + source

where ρ is the density, \vec{w} is the velocity vector, Φ the variable in question, Γ_Φ the diffusive exchange coefficient for Φ and S_Φ the source term (Bird, Stewart & Lightfoot, 1960). For our purpose, it is necessary to solve the momentum and continuity equations. In the momentum equation, the particular transport parameters are: $\Phi = u, v, w$ (velocity components), $\Gamma_\Phi = \rho(v_t + v_l)$ and $S_\Phi = -\frac{\partial p}{\partial x}$, where v_t and v_l are the turbulent and laminar viscosities. In the continuity equation, $\Phi = 1$ and $\Gamma_\Phi = S_\Phi = 0$.

The Navier-Stokes equations together with the continuity equation comprise a closed set of equations, the solution of which provides a valid description of laminar and turbulent flows. Turbulence fluctuations can generate

rates of momentum transfer far greater than those due to molecular diffusion. The turbulent motion has a wide spectrum of eddy sizes, and large and small eddies can coexist in the same volume of fluid. Several models were developed to define the turbulence, most of them using the eddy-viscosity concept ($\mu_t = \rho v_t$), which is a property of the local state of turbulence.

3. Constant-viscosity turbulence model

The turbulence model that uses a constant value for the eddy viscosity is the simplest one [2]. For dimensional reasons, the effective kinematic viscosity associated with the local turbulence is proportional to the typical velocity and to the characteristic length, given as:

$$v_t = C w l_c \quad (2)$$

Estimation of a reasonable value for v_t can be made by taking $C = 0.01$, typical velocity as the mean-flow velocity (the bulk value) and characteristic length as 10% of the flow width.

It is often convenient to use this simple model whilst the main features of the CFD simulation are being put together. Once the other aspects of the flow are well represented, a more accurate turbulence model can be activated.

4. k- ε turbulence model

The k- ε turbulence model has proved the most popular, mainly because it does not require a near-wall correction term [3-5]. The typical velocity is calculated from the solution of the transport equation for turbulent kinetic energy, k . The dependent variable of the second transport equation is not usually l_c itself, but rather the variable $k^m l_c^n$. The standard high-Re form of the k- ε model employs the following turbulence transport equations:

- *kinetic-energy equation*:

$$\frac{\partial}{\partial t}(\rho k) + \operatorname{div}(\rho \vec{w} k) = \operatorname{div}\left(\rho \frac{v_t}{\sigma_k} \operatorname{grad}(k)\right) + \rho(P_k + G_b - \varepsilon) \quad (3)$$

- *dissipation rate equation*:

$$\frac{\partial}{\partial t}(\rho \varepsilon) + \operatorname{div}(\rho \vec{w} \varepsilon) = \operatorname{div}\left(\rho \frac{v_t}{\sigma_\varepsilon} \operatorname{grad}(\varepsilon)\right) + \rho \frac{\varepsilon}{k} (C_1 P_k + C_3 G_b - C_2 \varepsilon) \quad (4)$$

where k is the kinetic energy of turbulence, ε is the dissipation rate, σ_k and σ_ε are effective Prandtl-Schmidt numbers [6].

The two-equation models account for the transport effects of velocity and characteristic length, and the model determines the distribution of the last. The

constant C_3 has been found to depend on the flow situation. It should be close to zero for stably-stratified flow, and close to 1.0 for un-stably-stratified flows.

P_k is the volumetric production rate of turbulent kinetic energy by shear forces and G_b (buoyancy production) is the volumetric production rate of turbulent kinetic energy by gravitational forces interacting with density gradients. G_b is negative for stably-stratified (dense below light) layers, so that k is reduced and turbulence damped. G_b is positive for un-stably-stratified (dense above light) layers, in which therefore k increases at the expense of gravitational potential energy.

The model forms a good compromise between generality and economy of use for many CFD problems.

5. Optimisation of an industrial dryer

The drying space of the full-scale unit has overall dimensions 3 x 2 x 6 m (width, height and length). Two rows of trays are placed symmetrically from the longitudinal vertical plane of the room. The length of one tray is 75 cm, and the width can be either 50 or 75 cm. Therefore, each row will have 12 columns by using 50 cm trays, and 8 columns by using 75 cm trays.

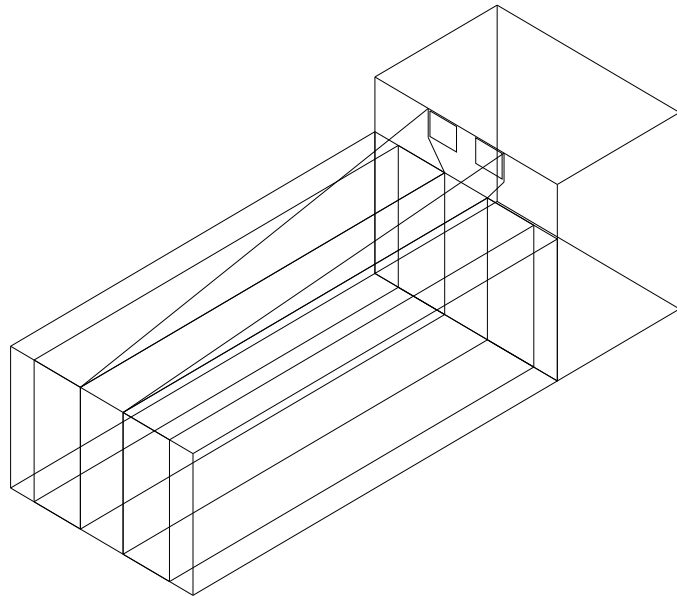


Fig. 1. Outline of the industrial dryer

The shelf system, constructed to support the trays, permits the adjustment of the distance between trays according to technological needs. One column can contain up to 25 trays. Above the drying room, in the direction of the longitudinal axis, there is a wedge shape distribution channel. Next to the drying space is the equipment room containing fans, heat exchangers, a burner and the control panel. The inlet and outlet openings for the drying air are on the back wall: the two inlets at the centre-upper part of the distribution channel, each of 44 cm width and 36 cm height, and the two outlets at the lateral-bottom sides of the drying room, each of 2 m height and 30 cm width (see *Figure 1*). An example of tray arrangement (with 14 trays per column) is given in *Figure 2*.

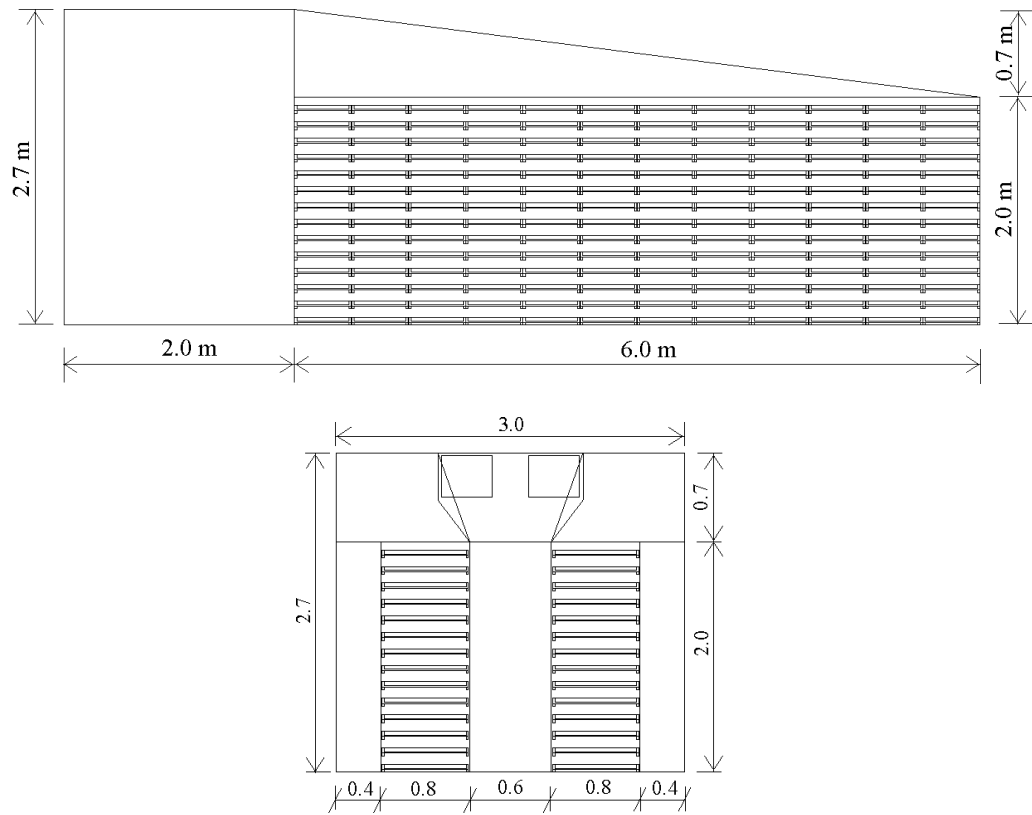


Fig. 2. Side and front view of the industrial dryer with 14 trays per column

The airflow inside this complicated geometry space was simulated with the PHOENICS CFD code. The computational domain (half of the space due to its longitudinal plane of symmetry) has the overall dimensions 1.5 x 2.7 x 6 m and was divided in 22320 cells as follows: 10 cells in x direction, 62 cells in y direction from which 50 cells for the drying room containing 25 trays and 12 cells for the distribution channel, and 36 cells in z direction. Therefore, each cell has 15 cm and 16.5 cm for x and z direction respectively, whereas in y direction has 24 mm for those cells corresponding to the tray thickness, 16 mm between the trays and 58 mm inside the distribution channel. The grid for the computational domain is given in *Figure 3*.

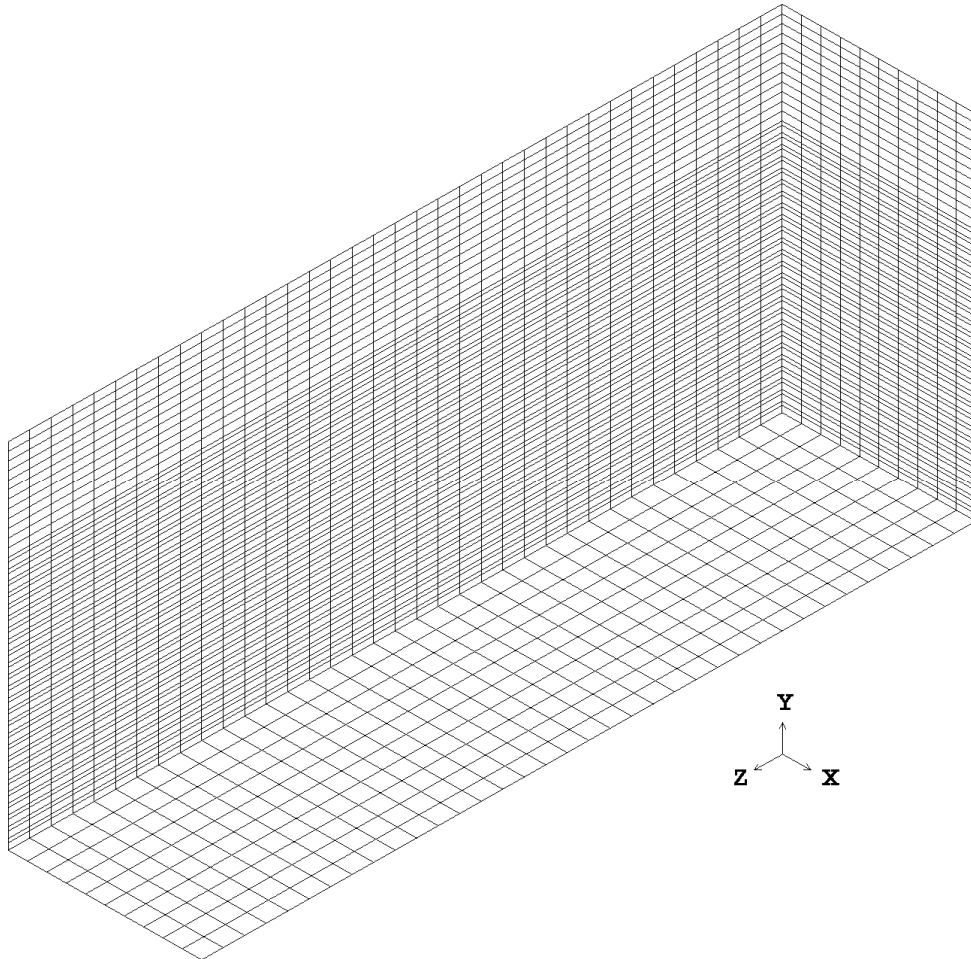


Fig. 3. Grid of the computational domain for 25 trays per column

Because the flow between the trays is horizontal, the velocity has only two components (in x and z directions) and the grid has only one cell between two trays. Each tray is considered to be a blockage for the flow. No-slip boundary conditions and appropriate wall functions apply on the solid surfaces. The selected turbulence model was the standard 2-equation $k-\epsilon$. For an inlet flow rate of 3.33 m^3/s , which corresponds to a mean inlet velocity of 21 m/s and a mean velocity over the trays of 2.86 m/s, a typical example of 3-D representation of the velocity vector distribution inside the drying room is given in *Figure 4*. It can be observed a non-uniform flow inside the drying space associated with re-circulation regions.

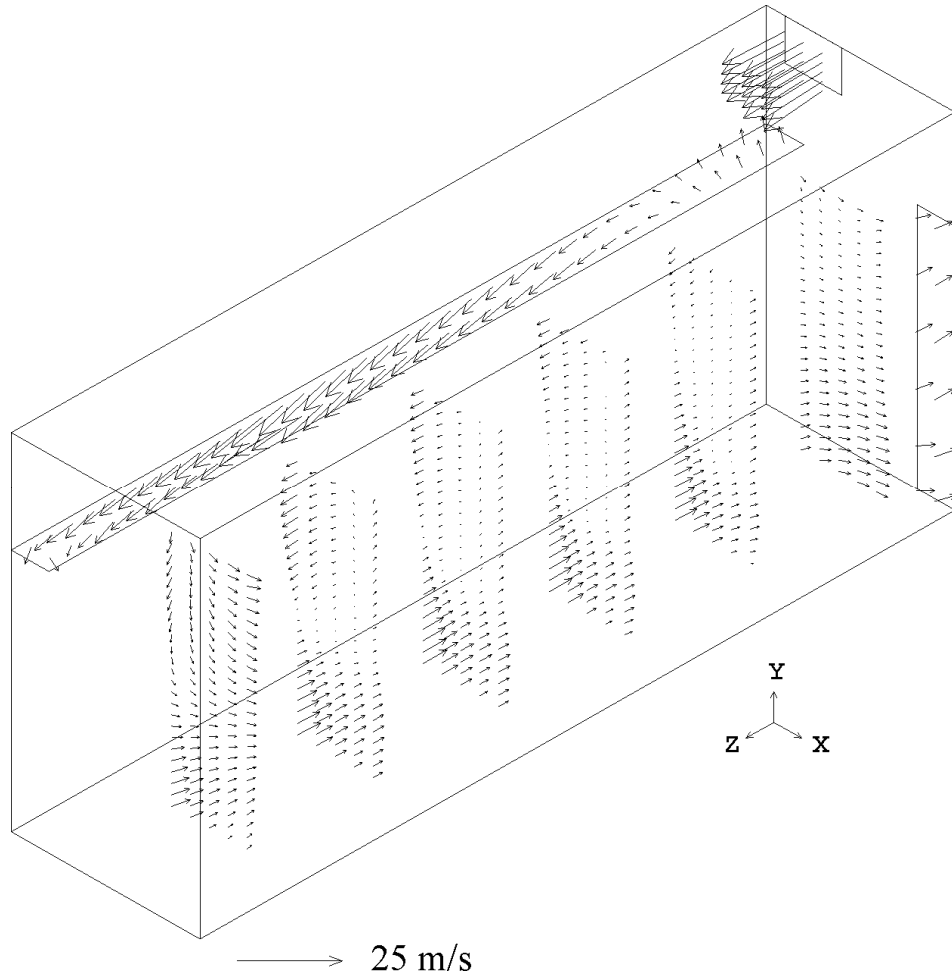


Fig. 4. 3-D velocity distribution inside drying room

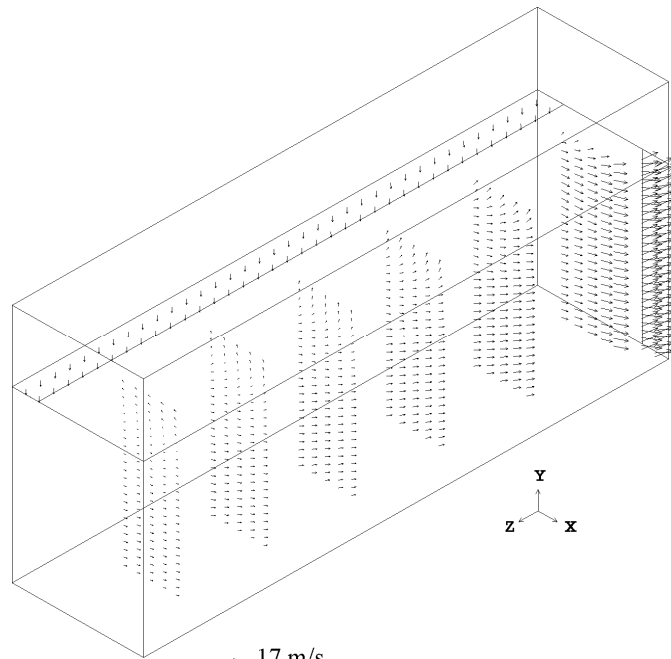


Fig. 5. 3-D velocity distribution in vertical planes after optimisation

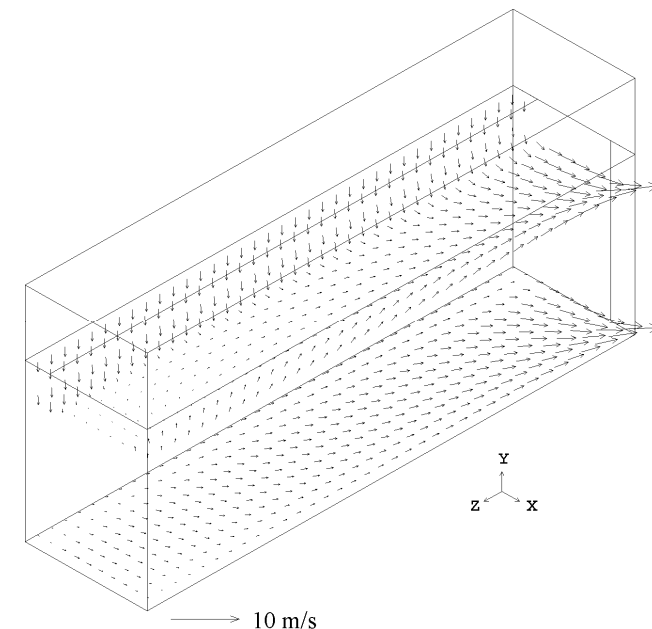


Fig. 6. 3-D velocity distribution in horizontal planes after optimisation

Graphical representations of the flow parameters for different geometrical configuration and their interpretation led to the optimisation of the tray arrangement, size and position of the inlet opening, opportunity of using separation walls between rows of trays and directing wings inside the distribution channel and central corridor. For example, the optimisation of the distribution channel geometry led to a uniform inlet air for the drying space, thus more uniform flow and no re-circulation are achieved between the trays as can be seen in *Figure 5* and *6*. An up-view of the flow above several trays (1st tray starts from the bottom) is presented in *Figure 7*. The proposed improvements were implemented into practice on an industrial dryer that operates in Kimi, Evia Island of Greece. The design improvements resulted from the numerical simulation led to an increment of 23% in the uniformity of the humidity inside the final product, when 3 tons of Corinthian grapes were dried during the monitoring period.

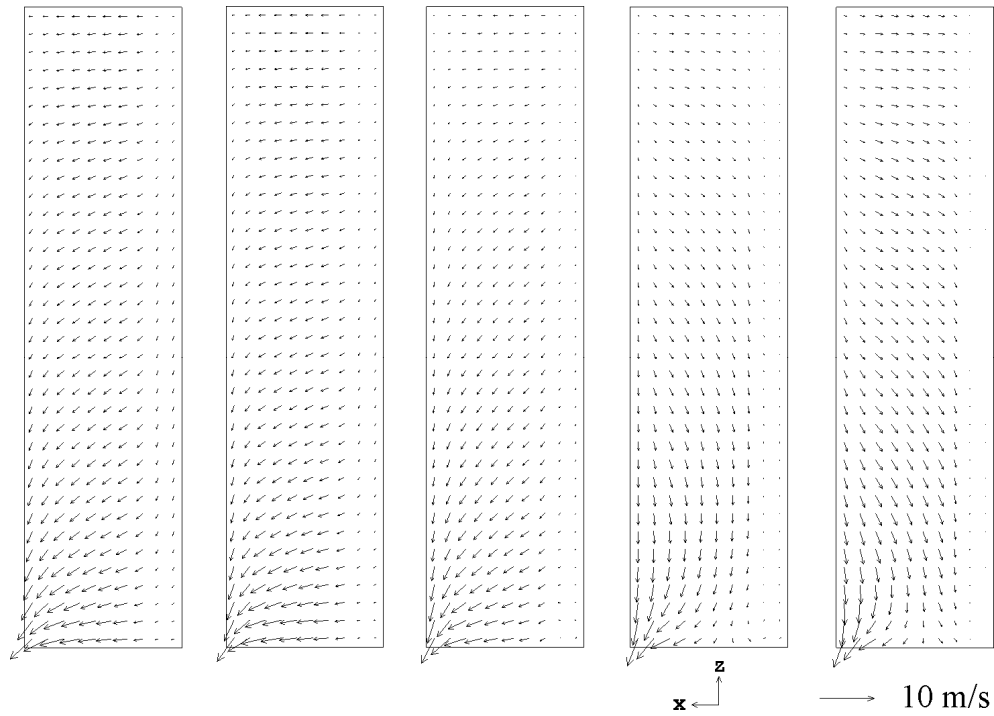


Fig. 7. 2-D velocity distribution for several trays (1st tray starts from the bottom)

6. Conclusions

The evaluation of the airflow parameters inside drying units is a very important task. In some cases, the air has to be removed, while in others, it just helps the separation of the other two phases. Experimental investigations give valuable information for the understanding of a specific phenomenon and help to validate general CFD codes that are afterward used to extensively analyse the phenomenon by numerical simulation. Improvement solutions by flow manipulation techniques using CFD codes can be given to both, dryers that are already in operation and new units under design.

B I B L I O G R A P H Y

- [1]. *A.-G. Ghiaus, D.P. Margaris, and D.G. Papanikas*, Improvement of food drying quality by flow manipulation techniques, Proceedings of Second Trabzon International Energy and Environment Symposium, Trabzon, pp. 359-362, 1998.
- [2]. *B.E. Launder, W.C. Reynolds, W. Rodi, J. Mathieu and D. Jeandel*, Turbulence models and their applications, Editions Eyrolles, 1984.
- [3]. *S. B. Pope*, Turbulent flows, Cambridge University Press, 2000.
- [4]. *C.K.G. Lam, and K.A. Bremhorst*, Modified form of k- ϵ model for predicting wall turbulence, ASME, Journal of Fluids Engineering, 103, 456-460, 1981.
- [5]. *F.R. Menter*, Two-equation eddy-viscosity turbulence models for engineering applications, AIAA Journal, 32-8, 1598-1605, 1994.
- [6]. *B.E. Launder and D.B. Spalding*, Mathematical models of turbulence, Academic Press, London, 1972.